Journal of Non-Crystalline Solids 622 (2023) 122653

Contents lists available at ScienceDirect

Journal of Non-Crystalline Solids

journal homepage: www.elsevier.com/locate/jnoncrysol

# Sol-gel synthesis of spherical monodispersed bioactive glass nanoparticles co-doped with boron and copper

M. Miola [a,b,*], E. Piatti [a], P. Sartori [a,c], E. Verné [a,b]

[a] Department of Applied Science and Technology, Politecnico di Torino, Institute of Materials Engineering and Physics, Corso Duca degli Abruzzi, 24, Torino, TO 10129, Italy
[b] PolitoBioMED Lab, Politecnico di Torino, Torino, TO 10129, Italy
[c] Instituto de Nanociencia y Materiales de Aragón (INMA), CSIC-Universidad de Zaragoza, Departamento de Física de la Materia Condensada, Zaragoza, 50009, Spain

ARTICLE INFO

*Keywords:*
Glass
Nanoparticles
Sol-gel
Bioactivity
Copper
Boron

ABSTRACT

In this work, an optimized sol-gel process for the synthesis of spherical and monodispersed bioactive glass nanoparticles doped with boron and copper was developed, by investigating different synthesis parameters. The obtained glasses were characterized in terms of morphology, composition, dispersibility, structure and *in vitro* reactivity. The performed characterizations demonstrated that shape, dimension and dispersion can be tailored by acting on the timing of the addition of the catalyst and on the synthesis process, in particular the centrifugation step. The optimized glass particles showed a spherical shape, good ions incorporation and good dispersion. *In vitro* bioactivity test demonstrated that the boron and copper addition did not interfere with the glass ability to induce the precipitation of hydroxyapatite. The shape, dispersion, bioactive behavior and content of boron and copper of these novel bioactive glass particles make them very promising for both hard and soft tissue engineering applications.

## 1. Introduction

Bioactive glasses (BGs) are a group of reactive materials, widely studied for their ability to bond to living tissues, generating a specific biological response by the living organism. Indeed, BGs are known for their ability of directly bonding to bone tissue through a biologically active interface layer of hydroxyapatite (HA), which is chemically equivalent to the mineral phase of the bone [1–3]. However, a variety of BG compositions are also investigated for applications in soft tissue engineering (TE) [4].

Conventionally, BGs are prepared using two main techniques, the melting technique, in which the glass is obtained by melting and quickly cooling a mixture of powdered solid precursors, and the sol-gel technique, in which a mixture of organic liquid precursors (the sol) is converted in a gel through reactions of hydrolysis and polycondensation, aging, drying, and calcination [5,6].

Various parameters affect the sol-gel process, such as initial precursors (type and number) [5–7], solvent (type and amount, related to solvent/alkoxide ratio (r) [6] and solvation degree), catalysts (type and amount) [5–7], temperature [7], gelation time [6], sol pH [7], capillary pressure [6], mixing mode [8], use of additives [7], and physical treatments [7], such as thermal treatments like aging and calcination [9].

According to the used catalyst, sol-gel methods can be divided into two main groups: basic-synthesis [10–12] and acid-synthesis [13,14]. Acid-base-co-catalysed methods are also applied to synthetize bioactive glasses, in particular in form of nanoparticles [15–17]. In addition, for the synthesis of spherical glass nanoparticles, a surfactant (e.g. P123 or CTAB) can be helpful by acting as template [18]. However, basic synthesis seems to be the most promising process to obtain individual particles [19].

Nowadays several sol-gel BG compositions are available, mainly based on the ternary system $SiO_2$ –$P_2O_5$–CaO [7], but the synthesis of monodisperse spherical BG nanoparticles (BGNs) is still an open issue. Indeed, the introduction of metal ions (e.g. $Cu^{2+}$, $Ag^{+}$) during the sol-gel synthesis of silica particles could impact the surface charge of the $SiO_2$ nanoparticles, leading to aggregation, inhomogeneity in size and irregular shapes of the final BG nanoparticles [10,20].

To address the previous issues, according to literature results, the experimental work reported in the present paper aims to tune sol-gel

* Corresponding author at: Department of Applied Science and Technology, Politecnico di Torino, Institute of Materials Engineering and Physics, Corso Duca degli Abruzzi, 24, Torino, TO 10129, Italy.
*E-mail address:* marta.miola@polito.it (M. Miola).

https://doi.org/10.1016/j.jnoncrysol.2023.122653
Received 29 June 2023; Received in revised form 14 September 2023; Accepted 23 September 2023
Available online 28 September 2023

glass synthesis, in order to optimize the size, shape and dispersibility of novel sol-gel BG particles containing boron (B) and copper (Cu), preliminarily investigated in a previous work by Piatti et al. [21]. All investigated syntheses are based on the co-solvent system water/ethanol because it is well-known that ethanol can act as dispersant [22]. Indeed, TEOS is not miscible in water, thus a second different solvent (usually an alcohol) is fundamental [5].

Based on authors' knowledge, there are no studies concerning the optimization of sol-gel synthesis to obtain spherical and well dispersed particles of bioactive glasses co-doped with B and Cu. Co-doping with B and Cu has been chosen due to the recognized angiogenic and antibacterial properties of this couple of ions, and the goal of developing spherical and monodispersed nanoparticles has been pursued in view of a potential use of the synthetized glass as dispersed phase in polymeric matrices for both hard and soft TE applications, that will be object of a further investigation.

## 2. Materials and methods

### 2.1. Materials

For the synthesis of bioactive glasses containing B and Cu, the following reagents were used:

- tetraorthosilicate (TEOS) $C_8H_{20}O_4Si$ at 99% (Sigma Aldrich), triethyl phosphate (TEP) $C_6H_{15}O_4P$ at 99% (Alfa Aesar), calcium nitrate tetrahydrate $Ca(NO_3)_2 \bullet 4\ H_2O$, copper nitrate trihydrate $Cu(NO_3)_2 \bullet 3\ H_2O$ (Fluka) and boric acid $H_3BO_3$ at 99% (Sigma Aldrich) as precursors for $SiO_2$, $P_2O_5$, CaO, CuO and $B_2O_3$, respectively;
- bi-distilled water and ethanol (EtOH, Sigma Aldrich) as solvents;
- nitric acid ($HNO_3$) at 70% (Sigma Aldrich) and ammonia solution $NH_4OH$ at 28–33% (Emsure) as catalysts.

### 2.2. Glass synthesis

A bioactive glass containing both B and Cu (SBCu), with nominal composition 62%$SiO_2$–9%$P_2O_5$–9%CaO-5%CuO-15%$B_2O_3$ (wt%) was synthetized by an improvement of the sol-gel process previously reported by the authors [21]. First of all, in this work a basic catalyst was used; although an initial low pH could help the formation of small nanoparticles, a low pH during the first stages of the synthesis process could also lead to particle aggregation [16]. In addition, the final pH of the sol was raised through the $NH_4OH$ (2 M) up to 12 because, according to some literature results [23], a higher pH can increase nanoparticles diameter and it is well known that a higher diameter helps to obtain monodisperse nanoparticles, being surface area and surface charge of bigger particles lower than in case of smaller particles. Moreover, this work was focused on the investigation of the influence of the addition method of ammonia solution and the addition of one or more centrifugation steps on the shape, dimensions, composition and dispersibility.

All syntheses were carried out using a "two-solutions method", i.e. a basic synthesis based on the initial mixture of two solutions, the first one containing EtOH and TEOS, whereas the second one containing only the solvents $H_2O$ and EtOH, and characterized by the addition of ammonia solution ($NH_4OH$ 28%) with the function of gelling agent. The syntheses are briefly described below and resumed in Table 1 and Fig. 1.

*Synthesis A* - modified synthesis reported in [21] avoiding the use of an acid catalyst and adopting the previously described "two-solutions method". A solution of EtOH and TEOS was mixed with a second solution containing $H_2O$ and EtOH for 30 min, creating a sol. Subsequently, all the other precursors (TEP, calcium nitrate, boron acid, copper nitrate) were added and mixed each 30 min. At the end of the mixing, NH OH 28% was introduced to allow particles formation. The suspension was dried for 48 h in a heater at 60 °C and calcined in the oven for 2 h at 700 °C with a slow temperature heating rate (5 °C/min).

In *Synthesis B*, a final centrifugation step (5 min at 7000 rpm) was added, before the drying step, in order to reduce the final liquid part and reduce the possibility of aggregation during

In *Synthesis C*, the ammonia was added at the beginning of the process, in the second solution with water and ethanol and the initial sol was centrifuged, removing almost all the liquid part, just after the formation of the silica nanoparticles, before the addition of the other precursors in order to reduce the final amount of liquid and the possibility of particle aggregation, while avoiding the removal of B and Cu ions. While in *Synthesis D,* a second centrifugation step was added at the end of the synthesis process, in order to remove as much liquid solution as possible before the drying step, further limiting the particles' agglomeration.

Taking into consideration size, shape, aggregation degree and ion incorporation, synthesis D was selected as the best one. Thus, samples of an undoped glass with the nominal composition of 77S (named S) were synthesized as control following the protocol of SBCu synthesis D, without the addition of B and Cu, in order to evaluate how the addition of such doping ions influences the glass properties.

**Table 1**
List of syntheses and adopted parameters.

| Synthesis | Addition time of the catalyst | Centrifugation |
|---|---|---|
| A | after the addition of all precursors | Absent |
| B | after the addition of all precursors | Final |
| C | included in one of the initial mixed solutions | Intermediate |
| D | included in one of the initial mixed solutions | Intermediate + Final |

### 2.3. Characterizations

#### 2.3.1. Morphological and compositional characterization

Morphological and compositional characterizations were performed using a field emission scanning electron microscope FE-SEM (Gemini SUPRATM 40, Zeiss, Germany), equipped with Energy Dispersion Spectrometry (EDS) device. To carry out the analysis, glass powders were attached to an aluminum stub using a double-side carbon tape and then sputtered with chromium for 100 s.

#### 2.3.2. DLS measurements

In order to evaluate their size distribution profile and their aggregation state, all synthetized BG nanoparticles were characterized using the dynamic light scattering (DLS, Anton Paar, Litesizer 500) technique.

The analysis was performed in water suspension at room temperature, after ultrasonication for 10 min.

DLS results together with SEM-EDS analyses were used for the preliminary characterization of all synthetized glasses, in order to evaluate the effect of the varied sol-gel parameters on particles dimension, aggregation state and composition, highlighting differences between the synthetized glasses and allowing to choose the best sol-gel synthesis among the tried syntheses. The selected glass particles were then further characterized with Brunauer, Emmett, Teller method (BET), Fourier-Transform Infrared Spectroscopy (FTIR), X-ray Diffraction (XRD) and *in vitro* bioactivity test as discussed later in the following paragraphs.

#### 2.3.3. BET measurements

BET measurements were carried out only on glasses synthesized with protocol D (SBCu from now on) and on its control glass (S). The analyser ASAP 2020 Plus (Micrometrics, United States) was used to perform the $N_2$ adsorption and desorption measurements and calculate the particle surface areas of the glass particles.

#### 2.3.4. FTIR analysis

In order to assess the structure of the selected glasses (SBCu and S), FTIR analysis was carried out using the Thermo Scientific Nicolet iS50 FTIR Spectrometer (equipped with OMNIC software) and KBr pellets (FTIR-KBr). The pellets were produced using 2 mg of glass and 150 mg of

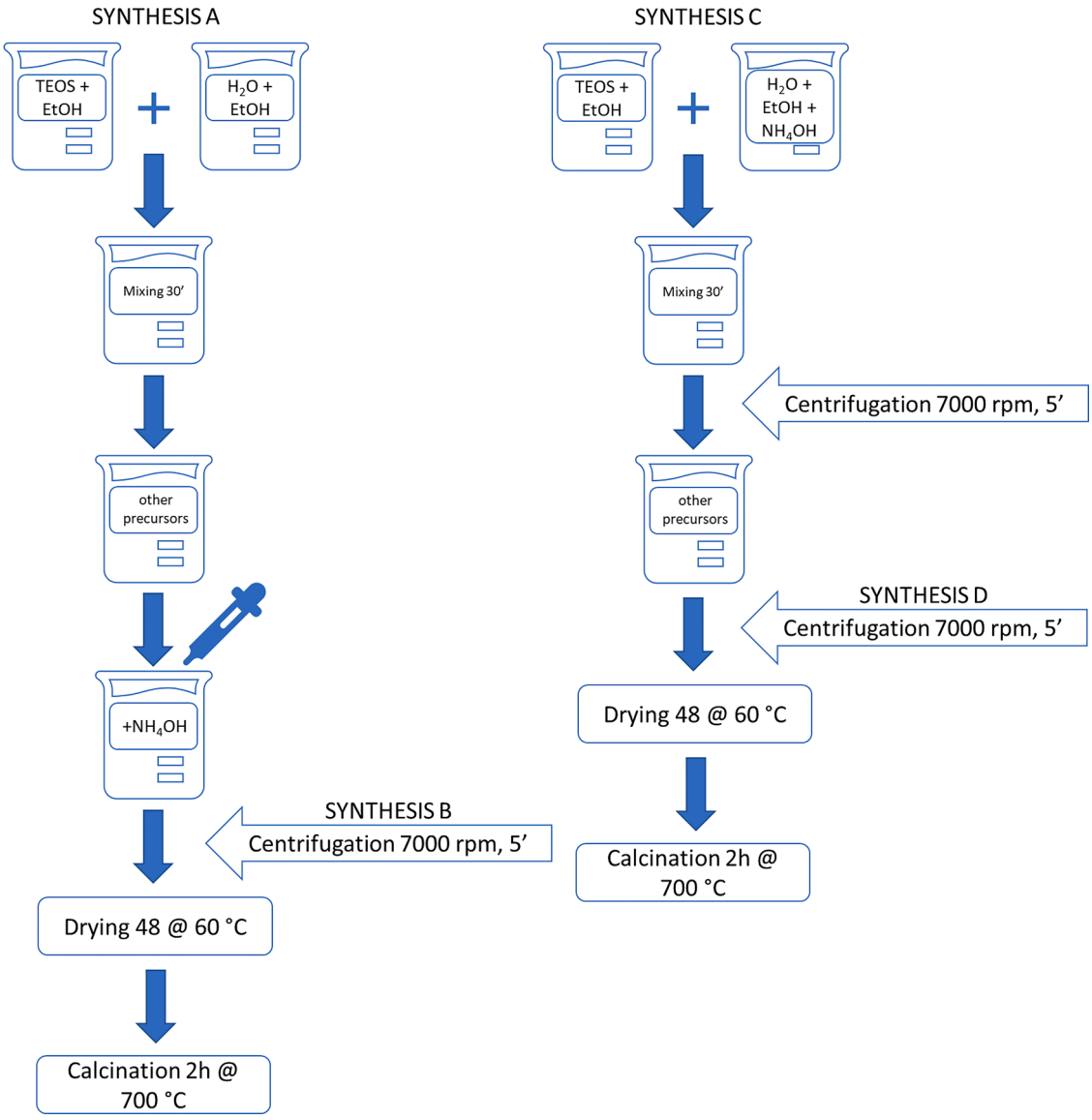


**Fig. 1.** Scheme of the performed syntheses.

KBr. The spectrometer was used in transmission mode with a chosen number of spectral scans equal to 32, a resolution of 4 $cm^{-1}$ and a wavenumber range between 4000 and 525 $cm^{-1}$.

### 2.3.5. *X-ray diffraction characterization*

The XRD analysis was performed in order to study the structure of the glasses. For the spectra measurements, the X'Pert Philips diffractometer was used, adopting the Bragg Brentano camera geometry and the Cu-Ka incident radiation, with a source voltage of 40 kV, a current of 30 mA, an incident wavelength λ of 1.5405 Å, a step size Δ(2θ) of 0.02° and a counting time of 1 s per step. The analysis degree 2θ was varied between 10° and 70°. The X'Pert HighScore program (equipped with PCPDFWIN database) was used for the spectra analysis.

### 2.3.6. *In vitro acellular bioactivity test*

The formation of a layer of HA on the surface of a BG can be induced *in vitro* by immersing the glass samples in a protein-free and acellular aqueous solution, which simulates the body fluid, being buffered at physiological pH and having a composition and a concentration of ions similar to those of the inorganic part of human plasma [24]. Hence, the first stages of *in vivo* bioactivity can be simulated *in vitro* through the immersion of the BG in a simulated body fluid (SBF), providing favourable hints about the mineralization and bone bonding ability of the studied glass [23]. The SBF solution was prepared according to the Kokubo protocol [24], by dissolving NaCl, KCl, $K_2HPO_4 \bullet 3H_2O$, $MgCl_2 \bullet 6H_2O$, $CaCl_2$, and $Na_2SO_4$ into bi-distilled water and buffering at pH 7.4 with tris (hydroxymethyl) aminomethane $(HOCH_2)_3CNH_2$ (TRIS) and hydrochloric acid (HCl).

The *in vitro* bioactivity assessments were carried out on SBCu and S glasses by reacting 100 mg of BG powders in 100 ml of SBF at 37 °C in an orbital shaker (IKA® KS4000i control) with a shaking movement rate of 120 rpm, according to the literature test parameters (ratio = 1:1, rpm = 120) [25], for different immersion time in order to evaluate time-dependent evolution of bioactivity. The test was performed in triplicate. Four different time points were considered: 1, 3, 7, and 14 days of immersion in SBF. At each time point, BG samples were removed from SBF, washed with bi-distilled water, centrifugated at 5000 rpm for 10 min, left drying at 37 °C in an incubator and finally analysed using SEM-EDS and XRD. During all bioactivity tests, the solution pH was monitored, measuring it with a pH-meter after 1, 3, 5, 7, 10, 12 and 14 days of immersion in SBF, which was not renewed along all bioactivity tests.

## 3. Results and discussion

### 3.1. Morphological and compositional characterization

For the synthesis of monodisperse spherical BG nanoparticles, avoiding the use of surfactants, it is necessary to find a good compromise between geometrical features, like shape and size (which depend on the amount and concentration of added ammonia solution) and aggregation of the particles, influenced by synthesis process steps.

Observing SEM micrographs (reported in Fig. 2) it is possible to notice that the use of two-solutions method allowed obtaining spherical particles; however, the addition of the ammonia at the end of the synthesis (Synthesis A and B), and the consequent late gelation of the sol leads to aggregated and irregular particles with very small diameter (about 50 nm). The addition of a centrifugation step at the end of the process (Synthesis B) seems to slightly decrease the agglomeration of the powders (Fig. 2B). However, it was observed that the supernatant removed showed a blue color, caused by the presence of many Cu ions in the removed liquid.

A clear improvement in the shape and in the dispersion has been obtained by introducing ammonia at the beginning of the process (Synthesis C and D). In particular, the use of ammonia immediately during the mixing of the two solutions and the transfer of the centrifugation step before the addition of TEP and other precursors led to bigger (about 500 nm), more spherical and slightly less interconnected particles. Moreover, the centrifugation step before the addition of the doping ions allowed to avoid the removal of ions (in particular Cu ions) from the solution.

The addition of a final centrifugation step at the end of the process in synthesis D (Fig. 2D) favored the formation of less interconnected particles, characterized by a decrease in the presence of necks (evidenced with arrows in Fig. 2C, synthesis C) without altering the spherical shape and size of the glass particles.

Concerning EDS analysis, all syntheses showed good ions incorporation if compared to theoretical composition (as reported in Table 2), with the exception of phosphorus (P) for syntheses B and D, which was slightly lower than the theoretical composition. However, the P amount was comparable with that observed for BG particles produced in our previous work [21], which was already proven to be bioactive. The EDS analysis did not allow to verify the amount of B; however, B introduction was confirmed by FTIR analysis.

Fig. 3 reports the FESEM-EDS analysis of the control glass (S), synthesized using the same steps of synthesis D (selected after the preliminary investigation), without the addition of B and C, used as glass control. The S glass particles are spherical with an average diameter (about 600 nm) and they are depleted of P and Ca similarly to SBCu particles.

### 3.2. DLS results

DLS measurements were performed on all synthetized glasses, and their results are reported in Table 3, in terms of hydrodynamic diameter and polydispersity index. DLS results were compared with SEM-EDS results in order to select the best synthesis. From these results, it could be observed that the use of a final centrifuge in syntheses where ammonia is added at the end of the process (Synthesis B) did not seem to

**Table 2**
EDS analysis: comparison of ions amount (at%) for glasses synthesized using different processes.

| Synthesis | Ions (at%) | | | |
|---|---|---|---|---|
| | Si | P | Ca | Cu |
| A | 77 ± 0.3 | 3 ± 0.1 | 14 ± 0.4 | 5 ± 0.3 |
| B | 77 ± 0.5 | 2 ± 0.4 | 16 ± 0.5 | 4 ± 0.3 |
| C | 74 ± 1.4 | 6 ± 0.4 | 14 ± 1.1 | 6 ± 0.8 |
| D | 82 ± 0.7 | 2 ± 0.1 | 10 ± 0.7 | 6 ± 0.6 |
| **Theoretical composition** | | | | |
| SBCu | 75 | 9 | 12 | 4 |

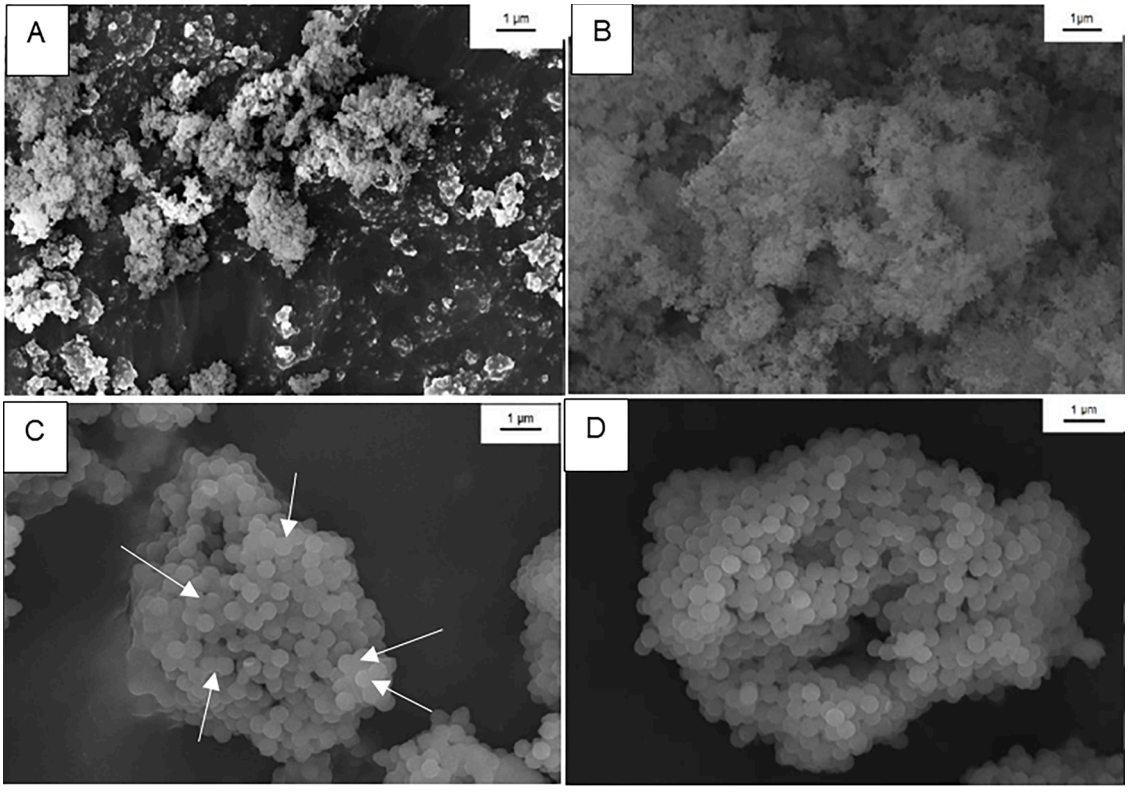


**Fig. 2.** FESEM micrographs (at 20 KX) of glasses synthetized through synthesis (A)–(D).

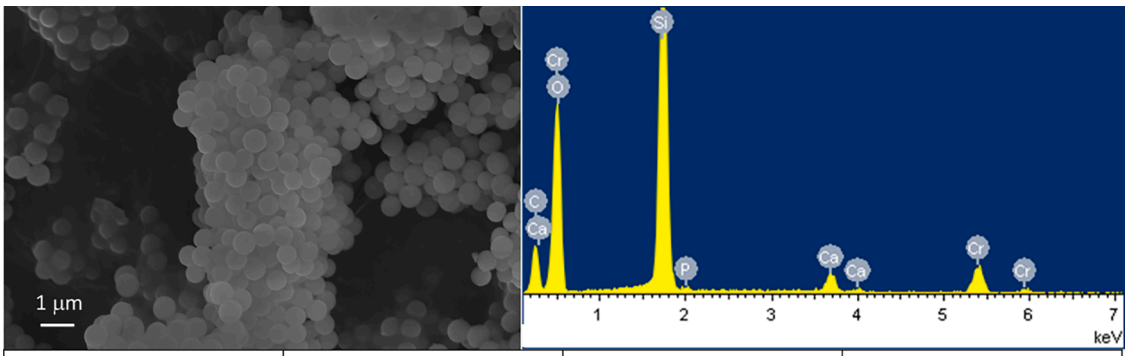


| Ions (at%) | Si | P | Ca |
|---|---|---|---|
| S glass | 90 ± 0.4 | 2 ± 0.1 | 8 ± 0.4 |
| Theoretical composition | 77 | 8 | 15 |

**Fig. 3.** FESEM-EDS analysis of S control glass, synthesized using the protocol of synthesis D.

**Table 3**
Hydrodynamic diameter and polydispersity index of all synthetized glasses.

| Synthesis | Hydrodynamic diameter [nm] | Polydispersity index |
|---|---|---|
| A | 663 nm | 30% |
| B | 785 nm | 38.4% |
| C | 3193 nm | 35.5% |
| D | 1557 nm | 26.8% |

have a significant influence on particle aggregation. On the contrary, in syntheses where ammonia is added at the beginning of the process, the addition of an intermediate centrifugation step (Synthesis C) and above all the addition of a second centrifugation (Synthesis D) seemed to be more effective in reducing the aggregation. Indeed, the glass particles synthesized with approach D showed the lowest hydrodynamic diameter (in comparison with the particles dimensions observed at FESEM) and polydispersity index. It should be underlined that, in any case, the diameter observed with the DLS analysis is higher than that measured with FESEM, due to the hydration layer present around the nanoparticles.

Therefore, based on the results obtained from the FESEM-EDS analyses and from the DLS, the synthesis D (SBCu) was considered the best one in terms of size, shape and dispersion.

### 3.3. BET measurements

BET measurements were carried out on the selected glass (SBCu, synthesis D) and its control glass (S). Surface area values are reported in Table 4. It is interesting to notice that the surface area clearly decreased with the addition of doping B and Cu ions. These results confirmed our previous observations on BGs with these same compositions but synthetized with different synthesis routes and they are in agreement with literature works that reported a decrease in BG surface area as a function of the incorporation of doping ions [10,20,26,27].

**Table 4**
Surface area values obtained with BET measurements for S and SBCu glasses.

| Surface area [$m^2/g$] | |
|---|---|
| S | 8.01 $m^2/g$ |
| SBCu | 2.52 $m^2/g$ |

### 3.4. FTIR analysis

The FTIR spectra of S and SBCu glasses are reported in Fig. 4. The more evident peaks in FTIR spectra of both glasses are the ones that can be noticed around 1200–1000 $cm^{-1}$ and the one at 800 $cm^{-1}$, which can be assigned to the Si-O-Si asymmetric [16,28] and symmetric stretching vibration [16,29], respectively.

For what concerns the FTIR spectrum of SBCu glass, apart for the peaks already analyzed for S glass, another evident peak can be noticed around 1600–1300 $cm^{-1}$ and attributed to the B-O bond stretching vibrations of triangular [$BO_3$] elementary units [30–32], and two smaller peaks at 942 $cm^{-1}$ and at 650 $cm^{-1}$, that can be attributed to B–O bond stretching vibrations of tetrahedral [$BO_4$] units [33] and borosiloxane bonds [32], respectively, in agreement with our previous literature results [21].

### 3.5. X-ray diffraction characterization

As shown in Fig. 5, the XRD pattern of both glasses, S and SBCu, are characterized by the typical broad halo between the 15° and 35°, due to the amorphous nature of the glasses, as already widely shown in previous literature works [34,35].

For what concern the pattern of SBCu, it is possible to observe the presence of a very small peak around 30°, which could be attributed to a calcium phosphate phase (reference code: 00–003–0605), while the

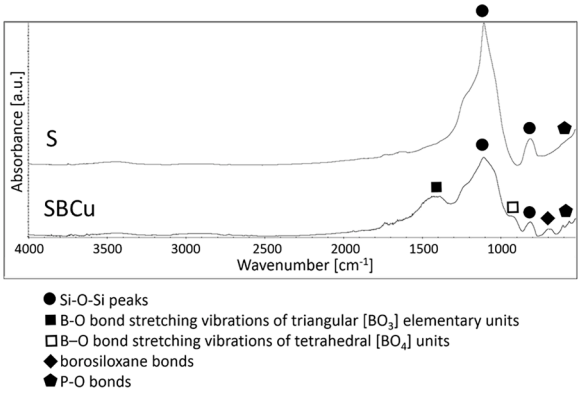


**Fig. 4.** FTIR spectra of S and SBCu glasses.

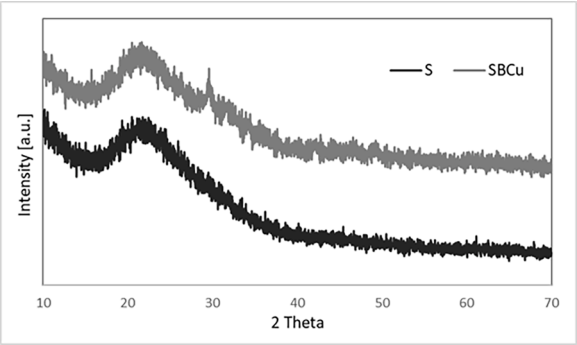


**Fig. 5.** XRD patterns of S and SBCu glasses.

pattern of undoped glass does not highlight crystallization peaks.

### 3.6. *In vitro* acellular bioactivity test

In order to evaluate the bioactivity of S and SBCu glasses, pH measurements, SEM-EDS and XRD analysis were carried out on the glass powders after immersion in SBF. Regarding pH, no significative variations were observed in the considered timespan, during which the pH values remain almost constant, slightly varying in the range 7.46–7.51 in the case of S and 7.39–7.45 in the case of SBCu. This flat trend is in contrast with most of the experimental results available in literature, showing a strong pH increase during immersion in SBF [10,36]. However, it is well known that pH values depend on the ions exchange between BG powders and SBF, in other words, they depend on the BG composition. Indeed, in agreement with literature works, including our previous studies on sol-gel B- and Cu-containing BG particles, B-containing glasses tend to show a flatter trend in pH values, and in general, lower pH values if compared to other BGs, probably because of the buffering effect of B, like in case of SBCu [37]. Another factor that could contribute to these stationary low pH values could be the low amount of P in both S and SBCu glasses [38,39]. Taking into consideration that rapid pH changes (related to ions burst release after contact with human fluids, as simulated by immersion in SBF) can be toxic for cells, especially if high pH values (higher than 8) are reached, this low stationarity can be considered as a positive characteristic of our glasses.

The exchange of ions between the BGs and the SBF regard mainly P and Ca, which tend to increase on the glass surface during immersion time, till a layer of crystalline HA is formed at the interface between glass and SBF. Similar variations were observed on both S and SBCu glasses. This increase was particularly evident in SBCu glass (as shown by EDS results in Fig. 6), especially in case of P ions, which were significative more just after one day of immersion in SBF and almost 6 times more after 7 days in SBF. Furthermore, it is worth mentioning that there was a decrease in Cu concentration immediately after the first day of soaking in SBF. This Cu release should not be ignored since it could influence the bioactive behavior, and the potential therapeutic and antibacterial properties of the here synthetized BGs. The higher bioactivity of SBCu, in comparison to the undoped S, can be, in fact, attributed to the presence of boron, that have already largely demonstrated to enhance glass bioactivity, but could be also be influenced by Cu presence. Literature results about Cu effect on BG bioactivity are still controversial.

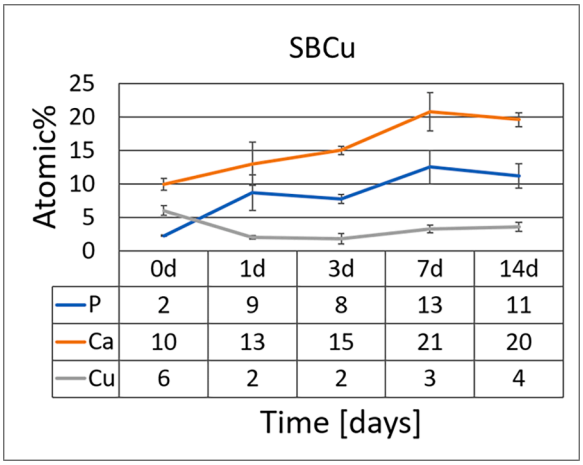


**Fig. 6.** EDS results of SBCu – P, Ca and Cu trends during immersion in SBF up to 14 days.

This increase in the amount of Ca and P was coherent with SEM images, which showed a significant difference in the surface morphology of S and SBCu particles after the immersion SBF solution (Fig. 7). SEM images evidenced the formation of the typical porous structure of *in vitro* HA crystals rich in Ca e P on the particles surface, as observed also by other authors [12].

The high bioactivity of SBCu glass was also confirmed by XRD (Fig. 8).

Indeed, the SBCu glass showed high bioactivity already after day 1 in SBF, as revealed by the numerous peaks attributable to HA, present in its XRD spectrum already after the first day of immersion. In particular, the peaks at about 26°, 28°, 32°, 34° and 53° can be ascribable to HA (reference code 00–001–1008), while the peak at about 31° is probably due to the presence of sodium chloride remaining in the powders even after washing.

## 4. Conclusions

An optimized sol-gel process for the synthesis of B and Cu doped spherical bioactive glass particles has been developed. In particular, the

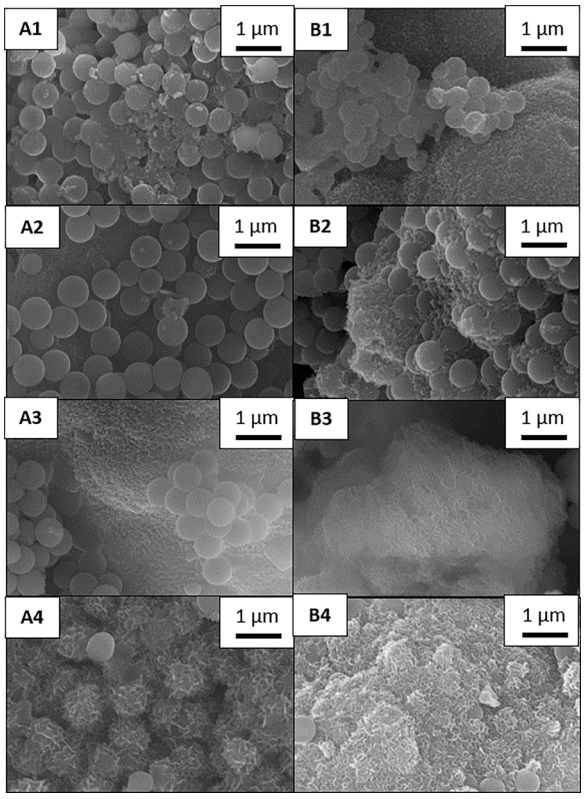


**Fig. 7.** SEM micrographs of BG particles immersed in SBF at 50 K X – S at day 1 (A1), day 3 (A2), day 7 (A3) and day 14 (A4), and SBCu at day 1 (B1), day 3 (B2), day 7 (B3) and day 14 (B4).

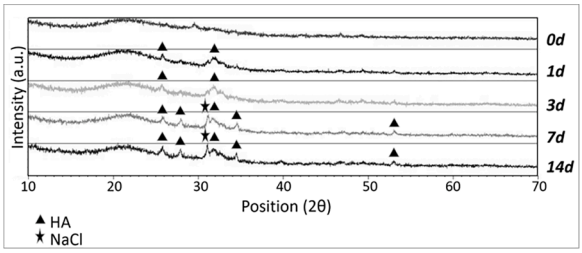


**Fig. 8.** XRD spectra of SBCu after 0d, 1d, 3d, 7d and 14 days in SBF.

effect of catalyst addition timing and centrifugation on particles size, shape, composition and distribution were investigated.

Comparing the obtained results, it can be assessed that the addition of $NH_4OH$ at the end of the synthesis and the consequent delayed gel formation led to aggregated, irregular and smaller particles; instead, the introduction of ammonia at the beginning of the synthesis, together with a centrifuge step before the addition of the precursors of P, Ca, B and Cu allows to synthesize less aggregated, spherical glass particles of about 500 nm in diameter. The addition of a second centrifuge step further improves the dispersibility of the particles, paving the way to their potential application as dispersed phase in polymeric matrices, for soft TE.

The sample that showed the best compromise in terms of shape, average size, dispersion and ion incorporation was selected and further characterized. The *in vitro* bioactivity test confirmed that this synthesis allowed the production of highly bioactive glass particles. Their bioactive behavior was enhanced with the incorporation of doping ions and not compromised by the presence of a crystalline phase in the amorphous network of SBCu glass. The bioactive behavior of this BGs compositions confirms the possibility of their application for bone TE. In conclusion, the synthesis of monodispersed B and Cu-doped glasses nanoparticles has been optimized, reducing their aggregation and enhancing their bioactivity. Therefore, the obtained glass nanoparticles (S and SBCu) are considered adequate for TE applications, in particular for both hard and soft TE applications where enhanced angiogenesis and antibacterial properties are requested. The incorporation of the optimized BGs nanoparticles into poly(ε-caprolactone) electrospun fibers is in progress and will be object of further investigation.

## CRediT authorship contribution statement

**M. Miola:** Conceptualization, Methodology, Investigation, Writing – original draft. **E. Piatti:** Investigation, Data curation, Writing – original draft. **P. Sartori:** Investigation, Data curation. **E. Verné:** Conceptualization, Supervision, Writing – original draft.

## Declaration of Competing Interest

The authors declare that they have no known competing financial interests or personal relationships that could have appeared to influence the work reported in this paper

## Data availability

Data will be made available on request.

## Acknowledgements

M. Miola and E. Piatti contributed equally to this work.

## References

[1] W. Cao, L.L. Hench, Bioactive materials, Ceram. Int. 22 (6) (1996) 493–507, https://doi.org/10.1016/0272-8842(95)00126-3.
[2] L.L. Hench, Bioceramics, J. Am. Ceram. Soc. 81 (7) (1998) 1705–1728, https://doi.org/10.1111/j.1151-2916.1998.tb02540.x.
[3] L.L. Hench, The story of bioglass®, J. Mater. Sci. Mater. Med. 17 (11) (2006) 967–978, https://doi.org/10.1007/s10856-006-0432-z.
[4] L.L. Hench, J.R. Jones, Bioactive glasses: frontiers and challenges, Front. Bioeng. Biotechnol. 3 (2015) 1–12, https://doi.org/10.3389/fbioe.2015.00194.
[5] A.E. Danks, S.R. Hall, Z. Schnepp, The evolution of "sol-gel" chemistry as a technique for materials synthesis, Mater. Horiz. 3 (2) (2016) 91–112, https://doi.org/10.1039/C5MH00260E.
[6] F. Baino, E. Fiume, M. Miola, E. Verné, Bioactive sol-gel glasses: processing, properties, and applications, Appl. Ceram. Technol. 15 (2018) 841–860, https://doi.org/10.1111/ijac.12873.
[7] G.J. Owens, R.K. Singh, F. Foroutan, M. Alqaysi, C.M. Han, C. Mahapatra, H. W. Kim, J.C. Knowles, Sol–gel based materials for biomedical applications, Prog. Mater. Sci. 77 (2016) 1–79, https://doi.org/10.1016/j.pmatsci.2015.12.001.
[8] D. Carta, J.C. Knowles, M.E. Smith, R.J. Newport, Synthesis and structural characterization of $P_2O_5$-CaO-$Na_2O$ sol-gel materials, J. Non-Cryst. Solids 353 (11–12) (2007) 1141–1149, https://doi.org/10.1016/j.jnoncrysol.2006.12.093.
[9] Y.F. Goh, A.Z. Alshemary, M. Akram, M.R. Abdul Kadir, R. Hussain, Bioactive glass: an *in-vitro* comparative study of doping with nanoscale copper and silver particles, Int. J. Appl. Glass Sci. 5 (3) (2014) 255–266, https://doi.org/10.1111/ijag.12061.
[10] A. Bari, N. Bloise, S. Fiorilli, G. Novajra, M. Vallet-Regí, G. Bruni, A. Torres-Pardo, J.M. González-Calbet, L. Visai, C. Vitale-Brovarone, Copper-containing mesoporous bioactive glass nanoparticles as multifunctional agent for bone regeneration, Acta Biomater. 55 (2017) 493–504, https://doi.org/10.1016/j.actbio.2017.04.012.
[11] K. Zheng, X. Dai, M. Lu, N. Hüser, N. Taccardi, A.R. Boccaccini, Synthesis of copper-containing bioactive glass nanoparticles using a modified Stöber method for biomedical applications, Colloids Surf. B Biointerfaces 150 (2017) 159–167, https://doi.org/10.1016/j.colsurfb.2016.11.016.
[12] Q. Nawaz, U.A.M. Rehman, A. Burkovski, J. Schmidt, A.M. Beltrán, A. Shahid, N. K. Alber, W. Peukert, A.R. Boccaccini, Synthesis and characterization of manganese containing mesoporous bioactive glass nanoparticles for biomedical applications, J. Mater. Sci. Mater. Med. 5 (64) (2018) 29–64, https://doi.org/10.1007/s10856-018-6070-4.
[13] V. Aina, C. Morterra, G. Lusvardi, G. Malavasi, L. Menabue, S. Shruti, C.L. Bianchi, V. Bolis, Ga-modified (Si-Ca-P) sol-gel glasses: possible relationships between surface chemical properties and bioactivity, J. Phys. Chem. C 115 (45) (2011) 22461–22474, https://doi.org/10.1021/jp207217a.
[14] A. Lucas-Girot, F.Z. Mezahi, M. Mami, H. Oudadesse, A. Harabi, M. Le Floch, Sol-gel synthesis of a new composition of bioactive glass in the quaternary system $SiO_2$-CaO-$Na_2O$-$P_2O_5$: comparison with melting method, J. Non-Cryst. Solids 357 (18) (2011) 3322–3327, https://doi.org/10.1016/j.jnoncrysol.2011.06.002.
[15] R.G. Furlan, W.R. Correr, A.F.C. Russi, M.R. da Costa Iemma, E. Trovatti, É. Pecoraro, Preparation and characterization of boron-based bioglass by sol–gel process, J. Sol-Gel Sci. Technol. 88 (1) (2018) 181–191, https://doi.org/10.1007/s10971-018-4806-8.
[16] A.A. El-Rashidy, G. Waly, A. Gad, A.A. Hashem, P. Balasubramanian, S. Kaya, A. R. Boccaccini, I. Sami, Preparation and *in vitro* characterization of silver-doped bioactive glass nanoparticles fabricated using a sol-gel process and modified Stöber method, J. Non-Cryst. Solids 483 (2018) 26–36, https://doi.org/10.1016/j.jnoncrysol.2017.12.044.
[17] A.M. El-Kady, M.M. Ahmed, B.M. Abd El-Hady, A.F. Ali, A.M. Ibrahim, Optimization of ciprofloxacin release kinetics of novel Nano-bioactive glasses: effect of glass modifier content on drug loading and release mechanism, J. Non-Cryst. Solids 521 (2019) 1–12, https://doi.org/10.1016/j.jnoncrysol.2019.119471.
[18] C. Vichery, J.M. Nedelec, Bioactive glass nanoparticles: from synthesis to materials design for biomedical applications, Materials 9 (4) (2016) 288, https://doi.org/10.3390/ma9040288.
[19] K. Zheng, A.R. Boccaccini, Bioactive glass nanoparticles: from synthesis to materials design for biomedical applications, Materials 9 (4) (2016) 288, https://doi.org/10.1016/j.cis.2017.03.008.
[20] H. Palza, B. Escobar, J. Bejarano, D. Bravo, M. Diaz-Dosque, J. Perez, Designing antimicrobial bioactive glass materials with embedded metal ions synthesized by the sol–gel method, Mater. Sci. Eng. C 33 (7) (2013) 3795, https://doi.org/10.1016/j.msec.2013.05.012.
[21] E. Piatti, E. Verné, M. Miola, Synthesis and characterization of sol-gel bioactive glass nanoparticles doped with boron and copper, Ceram. Int. 48 (10) (2022) 13706–13718, https://doi.org/10.1016/j.ceramint.2022.01.252.
[22] W. Xia, J. Chang, Preparation and characterization of nano-bioactive-glasses (NBG) by a quick alkali-mediated sol-gel method, Mater. Lett. 61 (3) (2007) 3251–3253, https://doi.org/10.1016/j.matlet.2006.11.048.
[23] M. Fandzloch, W. Bodylska, K. Roszek, D. Szymański, A. Jaromin, A. Lukowiak, Synthesis and characterization of sol–gel-derived $SiO_2$-CaO particles: size impact on glass (bio)properties, Part. Part. Syst. Charact. (2023), 2200184, https://doi.org/10.1002/ppsc.202200184.
[24] T. Kokubo, H. Takadama, How useful is SBF in predicting *in vivo* bone bioactivity? Biomaterials 27 (15) (2006) 2907–2915, https://doi.org/10.1016/j.biomaterials.2006.01.017.
[25] M. Magallanes-Perdomo, S. Meille, J.M. Chenal, E. Pacard, J. Chevalier, Bioactivity modulation of Bioglass® powder by thermal treatment, J. Eur. Ceram. Soc. 32 (11) (2012) 2765–2775, https://doi.org/10.1016/j.jeurceramsoc.2012.03.018.
[26] C. Wu, Y. Zhou, M. Xu, P. Han, L. Chen, J. Chang, Y. Xiao, Copper-containing mesoporous bioactive glass scaffolds with multifunctional properties of angiogenesis capacity, osteostimulation and antibacterial activity, Biomaterials 34 (2) (2013) 422–433, https://doi.org/10.1016/j.biomaterials.2012.09.066.

[27] H. Luo, J. Xiao, M. Peng, Q. Zhang, Z. Yang, H. Si, Y. Wan, One-pot synthesis of copper-doped mesoporous bioglass towards multifunctional 3D nanofibrous scaffolds for bone regeneration, J. Non-Cryst. Solids 532 (2020), 119856, https://doi.org/10.1016/j.jnoncrysol.2019.119856.

[28] A.M. El-Kady, A.F. Ali, R.A. Rizk, M.M. Ahmed, Synthesis, characterization and microbiological response of silver doped bioactive glass nanoparticles, Ceram. Int. 38 (1) (2012) 177–188, https://doi.org/10.1016/j.ceramint.2011.05.158.

[29] M. Mozafari, F. Moztarzadeh, M. Tahriri, Investigation of the physico-chemical reactivity of a mesoporous bioactive $SiO_2$-CaO-$P_2O_5$ glass in simulated body fluid, J. Non-Cryst. Solids 356 (28–30) (2010) 1470–1478, https://doi.org/10.1016/j.jnoncrysol.2010.04.040.

[30] H. Doweidar, G. El- Damrawi, M. Al-Zaibani, Distribution of species in $Na_2O$-CaO-$B_2O_3$ glasses as probed by FTIR, Vib. Spectrosc. 68 (2013) 91–95, https://doi.org/10.1016/j.vibspec.2013.05.015.

[31] I. Kashif, A. Ratep, Role of copper metal or oxide on physical properties of lithium borate glass, J. Mol. Struct. 1102 (2015) 1–5, https://doi.org/10.1016/j.molstruc.2015.07.070.

[32] W.C. Lepry, S.N. Nazhat, Highly bioactive sol-gel-derived borate glasses, Chem. Mater. 27 (13) (2015) 4821–4831, https://doi.org/10.1021/acs.chemmater.5b01697.

[33] E.E. Horopanitis, G. Perentzis, A. Beck, L. Guczi, G. Peto, L. Papadimitriou, Identification of the presence of crystalline phase in lithiated boron oxide ionic glass conductors, Mater. Sci. Eng. B Solid-State Mater. Adv. Technol. 165 (3) (2009) 156–159, https://doi.org/10.1016/j.mseb.2009.09.015.

[34] A. Bonici, G. Lusvardi, G. Malavasi, L.A. Menabue, Synthesis and characterization of bioactive glasses functionalized with Cu nanoparticles and organic molecules, J. Eur. Ceram. Soc. 32 (11) (2012) 2777–2783, https://doi.org/10.1016/j.jeurceramsoc.2012.02.058.

[35] J. Li, D. Zhai, F. Lv, Q. Yu, H. Ma, J. Yin, Z. Yi, M. Liu, J. Chang, C. Wu, Preparation of copper-containing bioactive glass/eggshell membrane nanocomposites for improving angiogenesis, antibacterial activity and wound healing, Acta Biomater. 36 (2016) 254–266, https://doi.org/10.1016/j.actbio.2016.03.011.

[36] S. Zhao, Y. Li, D. Li, Synthesis and *in vitro* bioactivity of CaO-$SiO_2$-$P_2O_5$ mesoporous microspheres, Microporous Mesoporous Mater. 135 (2010) 67–73, https://doi.org/10.1016/j.micromeso.2010.06.012.

[37] E. Mancuso, O. Bretcanu, M. Marshall, K.W. Dalgarno, Sensitivity of novel silicate and borate-based glass structures on *in vitro* bioactivity and degradation behaviour, Ceram. Int. 43 (15) (2017) 12651–71265, https://doi.org/10.1016/j.ceramint.2017.06.146.

[38] A.M. Abdelghany, H. Kamal, Spectroscopic investigation of synergetic bioactivity behavior of some ternary borate glasses containing fluoride anions, Ceram. Int. 40 (6) (2014) 8003–8011, https://doi.org/10.1016/j.ceramint.2013.12.151.

[39] S.M. Ahmadi, A. Behnamghader, A. Asefnejaad, Sol-gel synthesis, characterization and *in vitro* evaluation of $SiO_2$-CaO-$P_2O_5$ bioactive glass nanoparticles with various CaO/P2O5 ratios, Dig. J. Nanomater. Biostruct. 2 (3) (2007) 847–860.